*Materials Research*. 2024; 27:e20240143
DOI: https://doi.org/10.1590/1980-5373-MR-2024-0143

# Investigation the Effect of TiC on Some Properties of ZA-27 Alloy Prepared By Powder Metallurgy Method

***Asaad Kadhim Eqal*[a]*, *Jawdat Ali Yagoob*[b], *Haidar Akram Hussein*[c]**

[a]*Southern Technical University, Amarah Technical Institute, 62001, Amarah, Iraq.*
[b]*Northern Technical University, Engineering Technical College, Kirkuk, 36001, Iraq.*
[c]*Middle Technical University, Technical Engineering College-Baghdad, 10061, Baghdad, Iraq.*

Received: March 28, 2024; Revised: June 04, 2024; Accepted: June 09, 2024

The existing work is dedicated toward the manufacture of ZA-27/TiC as composites material via powder metallurgy. A mixture of Zn and Al with 63 and 27 wt%, respectively, is ball milled for 4 hrs at 145 rpm. Then, samples with disk-like shapes were made through pressing under 600 MPa and afterward sintered at 336 °C for 90 minutes in an electric furnace in argon gas. Other three groups from the above Zn and Al mixture ratio were prepared but with the addition of 3, 6, and 9 wt% TiC particles independently. The group's samples were prepared at the same conditions above. Hardness, density, and porosity microstructure observations, including optical and SEM-Mapping techniques were utilized to validate the effect of TiC particle additions with the listed above contents on the prepared ZA-27 alloy properties. The practical density of the prepared ZA-27 alloy is decreased basically owing to the used powder metallurgy route and with a lesser degree due to TiC addition. In contrast, the porosity is increased. But the hardness of the ZA-27 alloy is improved when TiC was added, and it was increased from 49.4 to 66 VHN with 0 to 9 wt% TiC addition. The optical microscope and SENM-Mapping facilities explained the distribution of co-existing Zn, Al, and TiC particles in the microstructures of the tested samples to improve the properties of ZA alloy.

**Keywords:** *NNCs, TiC particles, Hardness, Particulate strengthening, PM.*

## 1. Introduction

Zinc-aluminium (ZA) alloys have easily replaced cast iron, aluminum, and copper alloys in numerous fields since they have adequate mechanical and attractive tribological characteristics. But, lack of steadiness at higher temperatures makes them prone to failure even at 75 °C. The addition of ceramic additives has improved the properties of ZA alloy in a room and raised up temperatures[1]. Particulate reinforcement metal matrix composites (MMCs) can lead to an improvement in strength at significantly minor added costs than continuous reinforcements. The ZA-type alloys have become increasingly common among foundry zinc-based alloys utilized as matrix materials in recent years[2]. As journal-bearing materials for low-speed and heavy-load applications, ZA alloys are in advance for broad, profitable significance. The ZA-27 alloys have been used to replace (64 and 660) SAE bonzes in bearings, wear-resistant, bushings, and other applications due to their minor cost and equal or better-bearing efficiency[3]. Due to their unique features, particle-reinforced MMCs have received a lot of interest[4]. ZA MMCs reinforced with particulate ceramics have good corrosion and wear resistances, besides high specific strength modulus, and lesser friction coefficient[5]. Commercial ZA foundry alloys and Zn alloy matrix composites have been utilized for considerable industrial applications[6]. Compared to the liquid metallurgy route, such as the stir casting process, the powder metallurgy route has recently become an efficient production method in ZA-27 MMCs[7]. Therefore, it is a good way to improve their mechanical properties by introducing strong ceramic particles into the ZA-27 matrix alloy[8]. Girish et al.[9], Božić et al.[10], Kiran et al.[11], Naveen Kumari et al.[12], Shivakumar et al.[13], Bhaskar et al.[14], Folorunso and Owoeye et al.[15], Fatile et al.[16], Hashim et al.[17], and Kumar Yadav et al.[18], all the researchers listed above studied the ZA alloys prepared via the casting method. While few researchers have studied the ZA alloys fabricated by the PM method. Çelebi et al.[8] were investigated the mechanically milled and hot-pressed ZA-27/$Al_2O_3$ nano-composites. Their findings demonstrated that the nano-composites' tensile strength peaked at a milling time of 2 hours (163 MPa), after which it progressively decreased. Çelebi et al.[19], were studied in other work ZA-27/$Al_2O_3$-graphite hybrid nano-composite materials (HNMs) prepared by the PM method, including mechanical milling and hot-pressing (HP). The tensile strength, hardness, and density tests of HNMs were carried out. Pul et al.[20], were studied the effect of carbon nanotube (CNT) on the machinability of CNT-reinforced ZA-27 nano-composite. The value of hardness decreased, and the amount of porosity amplified with the rise in the CNT ratio in the composite matrix. Cutting forces and the surface roughness amounts increased with the increase in feed value. Using the simulation program ANSYS Fluent, Eqal and Yagoob[21], were investigated the numerical modeling of the solidification of ZA alloy castings. The aim of the present work is devoted to characterizing the micron size TiC addition on some structural and hardness properties of the ZA-27 alloy fabricated by PM.

*e-mail: asaad.kadhim@stu.edu.iq

## 2. Methodology

Zn powder with particles size range from 2 to 10 µm and 7.14 g/cm$^3$ tap density, Al powder with particle size range from 10 to 30 µm and 2.7 g/cm$^3$, and TiC powder with 4.93 g/cm$^3$ were used. China Jingan Chemicals & Alloy Company provided these powders. The chemical composition of the received powders is displayed in Table 1.

The powder mixture was introduced with 11mm diameter alloy steel balls with a Vickers microhardness number of 855 VHN measured by a Metkon microhardness tester with a 500 gm applied load in the mechanical engineering college laboratory-Tikrit University. Ball milling technique was applied in the current study to ensure better mixing and consolidation of the different use powders together. The powder charge to ball weight ratio was 1:10, respectively, and was put into 304 stainless steel containers; then, the charge was milled for 4 hours at 145 rpm. Ball-milled powders ( zn and Al) with TiC particle content ranging from 0 to 3, 6 and finally to 9 wt% were pressed into disc-like samples with a 15 mm diameter. Where a ball milling machine is designed and make for the current study with the aid of information obtained from Ugwuegbu et al.[22]. The uniaxial hydraulic press was used for the pressing step. The optimum applied pressing pressure was 600 MPa. According to the green density (ρg) the calculation Equation 1[23].

$$Pg = Mc / Vg \quad (1)$$

The theoretical density (ρTh) for green compacts (GCs) is measured according to Equation 2[13].

$$\rho Th = \Sigma\left(\rho Mi \times XMi\right) \quad (2)$$

Where: ρMi: ρ of (Zn, Al and TiC).
XMi: wt% of (Zn, Al and TiC).

Then, the green compacts (GCs) are sintered at 336 °C for 90 minutes in a carboline-type electric furnace under a continuous stream of argon gas from the beginning of sintering till room temperature. The rate of heating is fixed at 15 °C/min. The furnace turned off to cool the samples slowly inside it. The samples two faces were wet ground using SiC emery papers with (400, 1000, 2000 and 3000) grit then polished using suspension solution of 1µm alumina, washed with distilled water. The sintered compacts (SCs) samples were dried in LHT/60-type oven at 120 °C for half an hour. The SCs micro-hardness was measured with the same explained former process used for milling ball hardness measurement. The microstructure examination was performing via Optical microscopy, SEM-Mapping, and XRD analysis techniques to observe an evaluate the used powders shape and size and the microstructure of the SCs samples.

## 3. Results and Discussion

The picked up photos by SEM is explained the spherical shape of Zn powder particles in Figure 1. While, the Al powder particles shape was mainly hemispherical as shown in Figure 2. On the other hand the TiC powder particle shape was irregular bulky as shown in Figure 3.

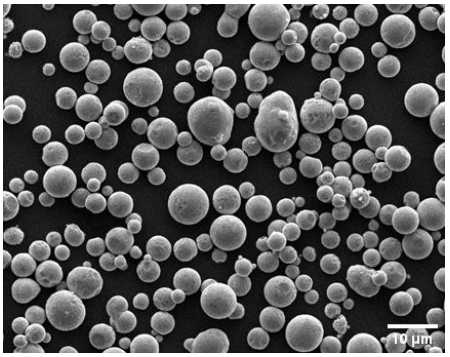


**Figure 1.** SEM image of Zn powder.

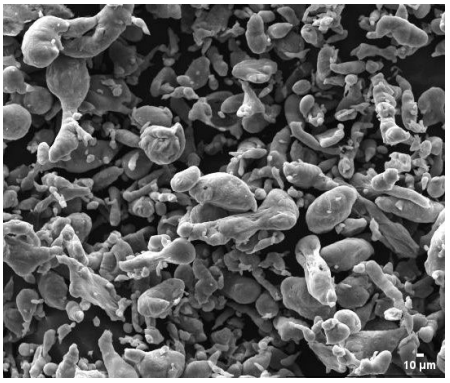


**Figure 2.** SEM image of Al powder.

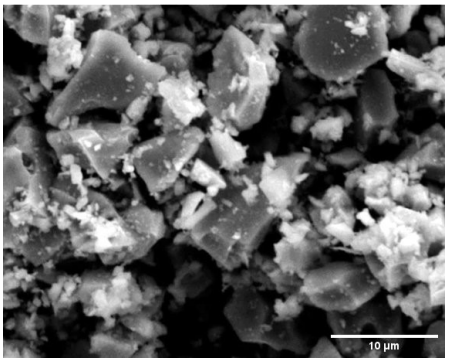


**Figure 3.** SEM image of TiC powder.

**Table 1.** Chemical composition of the used powders.

| Chemical Analysis of Zn | | | | | | | | | | |
|---|---|---|---|---|---|---|---|---|---|---|
| Zn | O | C | Pb | Cd | Fe | Mn | Na | Mg | Ca | K |
| >99.8 | <0.1 | <0.05 | 0.005 | 0.005 | 0.005 | 0.002 | 0.002 | 0.002 | 0.001 | 0.001 |
| Chemical Analysis of Al | | | | | | | | | | |
| Fe | Si | Cu | Ca | Al | | | | | | |
| 0.033 | 0.016 | 0.008 | 0.006 | Balance | | | | | | |
| Chemical Analysis of TiC | | | | | | | | | | |
| TiC | Fe | Ca | Mg | Cu | Mn | Na | Co | Ni | Si | S |
| 99.9 | 0.001 | 0.001 | 0.001 | 0.001 | 0.001 | 0.001 | 0.001 | 0.001 | 0.002 | 0.001 |

XRD resulted in the analysis diagram in Figure 4, ensuring the purity of the used TiC powder to prepare composite samples. The TiC powder XRD analysis results by mean of (2Θ) and intensity (I) values are well matched with CAS registry no. 12070-08-5 listed in the NBS monograph 25-section 18 and with (JCPDS, file No. 03-065-8417)[24]. The hkl of the peaks (111), (200), (220), (311), (222), (400), and (420) indicate that the TiC powders which are also ensure by other references. The purpose of the using XRD is to ensure that the tic powder with no impurities. This is detect of powder exactly Tic only.

The optical microscope image in Figure 5A for polished non-etched ZA-27 sintered compact sample explains the distribution of spherical smaller size Zn particles between larger Al powder particles without any segregation. On the other hand, black- colored pores relatively regular in shape (because of the used powder particular the base powder for zinc have regular shape therefore the remained pores between the boundaries of these powders will appear relative regular) appeared in the microstructure as it is pointed out by red circles. Where the create pores between the mixture powders particles appeared as dark areas. A part of these pores refers to the gaps that remained between powders' mixture boundaries after the pressing and sintering process. While some of these pores formed from the fragmentation of zinc particles from their positions due to grinding and polishing processes (which were made to prepare the samples for the microscopic examination) left behind them dark spherical with large pores near in their size to the zinc particles size[25]. Optical microscope photos revealed the relative progress in the polished samples' appearance and color by increasing TiC addition to the ZA-27 matrix as displayed in Figure 5B, C, and D). Where, the appearance of the dark color particles of TiC within the microstructure between aluminum particles and the dark area fraction was decreased by increasing the TiC particles content from (0 to 3, 6, and finally to 9) wt%. Also, the fractured TiC ceramic particles due to pressing pressure are embedded as very small fragments, particularly within softer aluminum particles.

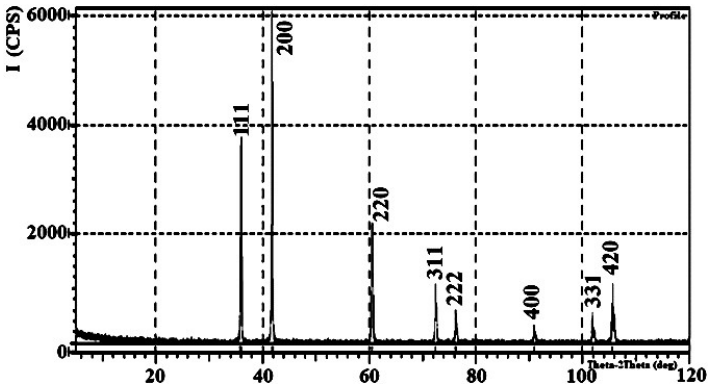


**Figure 4.** XRD analysis of TiC powder.

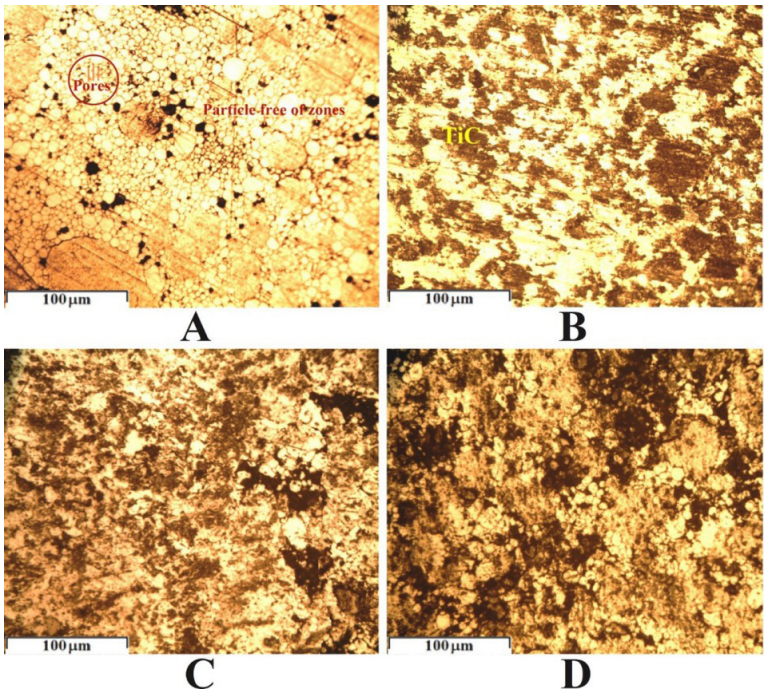


**Figure 5.** Optical microscope images for ZA-27 alloy and its composites, A. 0 wt% TiC, B. 3 wt% TiC, C. 6 wt% TiC, D. 9 wt% TiC.

For more explanation, an SEM facility was applied to observe the surface of the composite samples. Figure 6 shows the differences in the colors, size and distribution more clearly than in optical microscope photo images. Al particles appeared as dark grey in color, while Zn particles appeared as light grey in color.

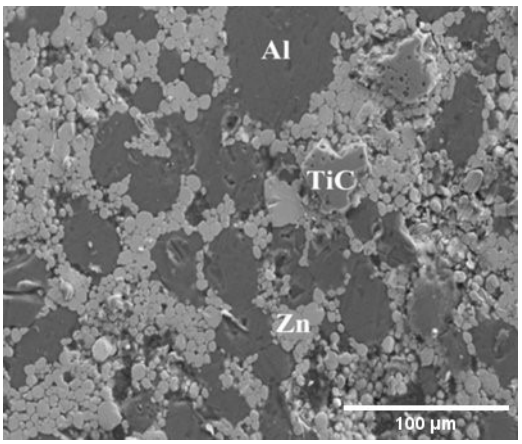


**Figure 6.** SEM image ZA-27/TiC composite.

The SEM-Mapping technique was used to ensure the existence and distribution of Al, Zn, and TiC particles. This is well defined in Figure 7. TiC particle distribution is detected as Ti and C elements. For more accurate observation of the TiC distribution within Al particles, a part of the image in Figure 8A is enlarged, as shown in Figure 8B. Also, Figure 8A is enhanced with the image for Ti element distribution, as displayed in Figure 8C. accordingly the two Figures 8B and C illustrate how a small particles of Ti with green color are embedded within Al powder particles This is a proof of TiC particles' distribution at Al and Zn particles boundaries and embedded within those softer particles as tiny fragments.

The theoretical density, as expected, is that the addition of TiC powder to the Zn and Al powders mixture tends to slightly decrease it. Where it decreased from 5.93 gm/cm$^3$ with zero TiC content to a lower amount reached 5.84 gm/cm3 at the higher TiC addition that is 9 wt%. This is well explained in Figure 9. But practically, when the ZA-27 samples without TiC addition are prepared by the PM process the measured density is decreased to 4.66 gm/cm3 from the calculated 5.93 gm/cm$^3$ theoretical density. The reason is due to the accompanied porosity which commonly occurs during utilizing PM in the manufacturing process.

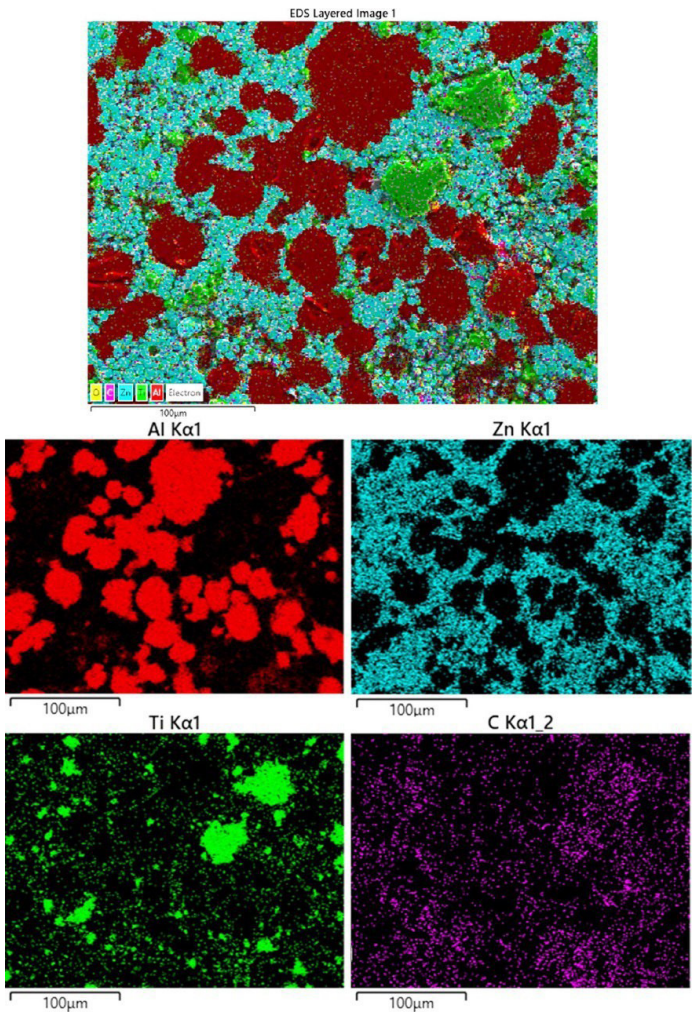


**Figure 7.** SEM-Mapping image ZA-27/TiC composite.

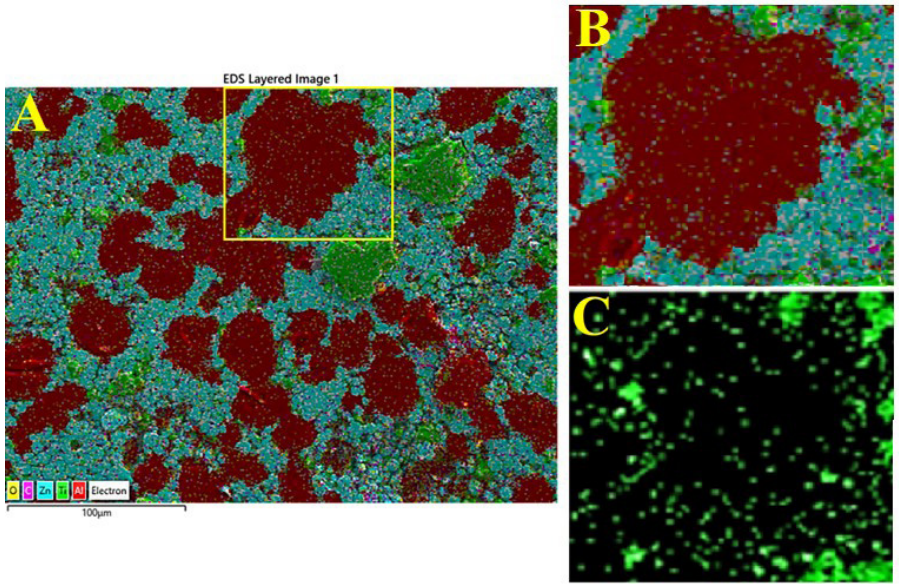


**Figure 8.** Explanation of TiC particle in the matrix of ZA-27/ composite with aid of SEM-Mapping facility.

The real porosity source is divided into open pores, where some of them appeared at the surface of the ZA-27 samples, as explained in Figure 5A, while the other is closed pores between the pressed and sintered mixture of Zn and Al powders particles. This in turn tends the practically measured density appear lower than the calculated theoretical one as is well illustrated in Figure 9. The addition of the TiC particles tends to further decrease the practically measured density of the ZA-27/TiC composite samples. This result is logically accepted and interpreted because a reasonable amount of associated porosity that existed between TiC particles will remain even after completing the sintering process. The sintering process is not able to eliminate the presented pores between TiC particles. The reason is the absence of diffusion processes between the TiC particles where they are ceramic material in which no ability of atoms diffusion. The phenomena which occur mainly between metallic powders particles to an extent. Accordingly, the practical density decreased to (4.41, 4.29, and 4.16) gm/cm$^3$ by (3, 6, and 9) wt% TiC addition, respectively, as it displayed in Figure 9.

The difference between the theoretical and practical densities results is also expressed as relative density which is in turn shown as percentage porosity that was increased by increasing the TiC addition to the ZA-27 matrix as displayed in Figure 10. It is essential to say that the accompanied porosity due to the utilization of the PM process to prepare the ZA-27 sample was 21.37% with zero TiC addition and increased to its maximum value of 28.78% when the maximum addition of about 9 wt% TiC was added. Hence, the maximum contribution of 9 wt% TiC addition in total percentage porosity increasing was 25.576%. Thus, the greater porosity occurrence belongs to the utilized PM route and, secondly, to the addition of the TiC ceramic particles. It is known that the hardness of ZA-27 alloy is arranged between 53-56 HB[21], which is equal to or very near to its VHN value. Hence the obtained 49.4 VHN value in the present work is well accepted according to the little drop in its value with

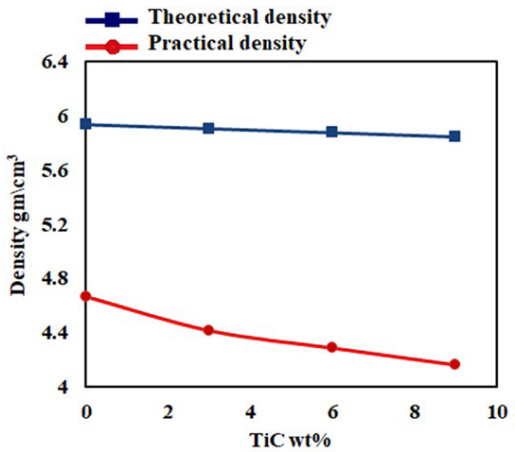


**Figure 9.** Shows the relative and theoretical density of ZA-27 alloy with TiC powder additives to it.

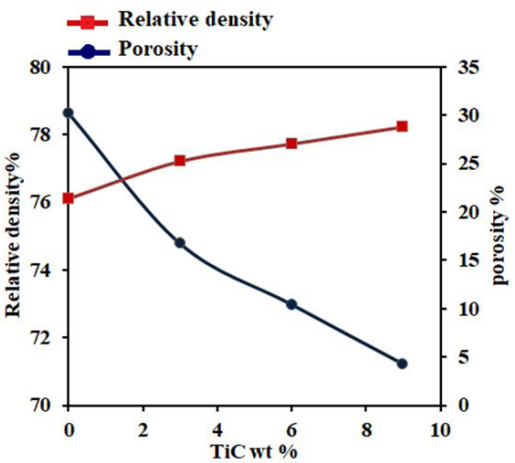


**Figure 10.** Shows the Relative density of ZA-27 matrix alloy and porosity with TiC powder additive in the matrix.

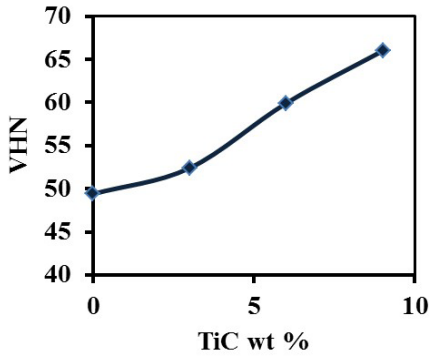


**Figure 11.** shows the hardness of the ZA27 matrix alloy with TiC powder additive in the matrix.

respect to the referred to (53-56) hardness number. Rather, the less measured microhardness (VHN) values revealed a continual increase with TiC addition to the ZA-27 matrix, as shown in Figure 11. The VHN of the ZA-27 matrix samples increased from 49.4 to 52.4, 59.93, and 66 by (3, 6, and 9) wt% TiC addition, respectively.

Thus TiC particles played a beneficial role in the strengthening of the ZA-27 matrix by particulate strengthening mechanism.

## 4. Conclusions

The most significant conclusions obtained for the prepared TiC-reinforced ZA-27 alloy by the PM method are listed below:

1. The accompanied porosity due to the utilization of the PM process to prepare the ZA-27 sample was 21.37% with zero TiC addition and increased to its maximum value of 28.78% when the maximum addition of about 9 wt% TiC particles was added.
2. Two factors are contributed in The occurrence of the porosity in the prepared ZA-27 alloy and its composites was approximately 75%. Which is mainly due to the utilized powder metallurgy route, and with lower contribution of TiC Particle?
3. TiC particles played a beneficial role in the strengthening of the ZA-27 matrix by particulate strengthening mechanism. This is clearly defiend with the improvement of the hardness of ZA-27 TiC addition.
4. Optical microstructure and SEM-Mapping observations are well explaining the good distribution of the mixed and milled powders mixtures in the Structure with no unacceptable segregations.

## 5. Acknowledgments

This research is fully supported by the Southern Technical University / Amarah Technical Institute.

## 6. References

1. Pola A, Tocci M, Goodwin FE. Review of microstructures and properties of zinc alloys. Metals. 2020;10(2):253. http://doi.org/10.3390/met10020253.
2. Gurumurthy O, Venkateswaran S. Experimental studies and regression analysis on mechanical properties of MMCs based zinc-aluminium alloys with graphite particles reinforcement. Mater Today Proc. 2022;49(Part 3):913-8.
3. Sharma S, Girish BM, Kamath R, Satish BM. Graphite particles reinforced ZA-27 alloy composite materials for journal bearing applications. Wear. 1998;219(2):162-8.
4. Singh L, Singh B, Saxena K. Manufacturing techniques for metal matrix composites (MMC): an overview. Adv. Mater Process Technol. 2020;6(2):441-57.
5. Sastry S, Krishna M, Uchil J. A study on damping behaviour of aluminite particulate reinforced ZA-27 alloy metal matrix composites. J Alloys Compd. 2001;314(1-2):268-74.
6. Li Z-Q, Zhou H, Luo X, Wang T, Shen K. Aging microstructural characteristics of ZA-27 alloy and SiC/ZA-27 composite. Trans Nonferrous Met Soc China. 2006;16(1):98-104.
7. Owoeye SS, Folorunso DO, Oji B, Borisade SG. Zinc-aluminum (ZA-27)-based metal matrix composites: a review article of synthesis, reinforcement, microstructural, mechanical, and corrosion characteristics. Int J Adv Manuf Technol. 2019;100(1-4):373-80.
8. Çelebi M, Çanakçi A, Özkaya S, Karabacak AH. The effect of milling time on the mechanical properties of ZA27/$Al_2O_3$ nano-composites. Univ J Mater Sci. 2018;6(5):163-9. http://doi.org/10.13189/ujms.2018.060504.
9. Girish B, Prakash KR, Satish BM, Jain PK, Prabhakar P. An investigation into the effects of graphite particles on the damping behavior of ZA-27 alloy composite material. Mater Des. 2011;32(2):1050-6.
10. Božić D, Stašić JM, Rajković VM. Microstructures and mechanical properties of ZA27-$Al_2O_3$ composites obtained by powder metallurgy process. Sci Sinter. 2011;43(1):63-70.
11. Kiran T, Kumar MP, Basavarajappa S, Vishwanatha B. Mechanical properties of AS-CAST ZA-27/Gr/SiCp hybrid composite for the application of journal bearing. J Eng Sci Technol. 2013;8(5):557-65.
12. Naveen Kumari ME, Bhaskar HB, Kiran TS. Characterization of Za-27 alloy reinforced with MgO particles by stir casting technique. J Eng Sci Technol. 2015;2(10):37-9.
13. Shivakumar N, Vasu V, Narasaiah N, kumar S. Synthesis and characterization of nano-sized $Al_2O_3$ particle reinforced ZA-27 metal matrix composites. Procedia Mater Sci. 2015;10:159-67.
14. Bhaskar S, Hemanth K, Jayasimha S. Mechanical characterization of ZA-27 reinforced with SiC p MMCs. In: International Conference on Current Trends in Engineering, Science and Technology; 2017; Bangalore, India. Proceedings. New York: Curran Associates, Inc.; 2017. p. 228-32.
15. Folorunso DO, Owoeye SS. Influence of quarry dust-silicon carbide weight percentage on the mechanical properties and tribological behavior of stir cast ZA-27 alloy based hybrid composites. J King Saud Univ Eng Sci. 2017;31(3):280-5.
16. Fatile B, Adewuyi B, Owoyemi H. Synthesis and characterization of ZA-27 alloy matrix composites reinforced with zinc oxide nanoparticles. Eng Sci Technol. 2017;20(3):1147-54. http://doi.org/10.1016/j.jestch.2017.01.001.
17. Hashim FA, Abdulkader NJ, Hisham KF. Fabrication and wear properties of ZA-27 alloy matrix hybrid composite reinforced with nanoparticles. Al-Qadisiyah J Eng Sci. 2018;11(4):446-54.
18. Kumar Yadav S, Kumar GK, Prakash RV. Preparation and characterization of ZA27-alumina-graphite reinforced hybrid composites. Mater Today Proc. 2019;18:57-65.
19. Çelebi M, Güler O, Çanakçı A, Çuvalcı H. The effect of nanoparticle content on the microstructure and mechanical properties of ZA27-$Al_2O_3$-Gr hybrid nano-composites produced by powder metallurgy. J Compos Mater. 2021;55(24):3395-408.
20. Pul M. The effect of carbon nanotube amount in machining of ZA-27 matrix carbon nanotube reinforced nano composite. Mater. 2022;27(2):e13226.

21. Eqal AK, Yagoob JA. Prediction of the solidification mechanism of ZA alloys using Ansys fluent. J Appl Sci Eng. 2021;24(5):699-706.
22. Ugwuegbu CC, Ogbonna AI, Ikele US, Anaele JU, Ochiezeand UP, Onwuegbuchulam A. Design, construction and performance analysis of a 5 kg laboratory ball mill. Global J Res Eng A. 2017;17(2):26-42.
23. Yagoob JA, Abbass MK. Characterization of cobalt based CoCrMo alloy fabricated by powder metallurgy route. In: 2nd International Conference for Engineering, Technology and Sciences of Al-Kitab (ICETS); 2018; Karkuk, Iraq. Proceedings. New York: IEEE; 2018.
24. Ali Abd N, Ali Yagoob J, Razeg KH. The effect of micro and nano size TiC additions on some properties of copper fabricated by powder metallurgy. J Nanostruct. 2021;11(3):588-600.
25. Dobrzański LA, Dobrzański LB, Dobrzańska-Danikiewicz AD. Overview of conventional technologies using the powders of metals, their alloys and ceramics in Industry 4.0 stage. J Achiev Mater Manuf Eng. 2020;98(2):56-85.